



The subunit assembly state of the Mediator complex is nutrient-regulated and is dysregulated in a genetic model of insulin resistance and obesity

Received for publication, February 1, 2019, and in revised form, April 18, 2019. Published, Papers in Press, April 26, 2019, DOI 10.1074/jbc.RA119.007850

Dou Yeon Youn^{‡§1}, **Alus M. Xiaoli**^{†¶}, **Hyokjoon Kwon**^{||}, **Fajun Yang**^{‡¶**}, and **Jeffrey E. Pessin**^{‡§**2}

From the Departments of [‡]Medicine, [¶]Developmental and Molecular Biology, and [§]Molecular Pharmacology and the ^{**}Fleischer Institute of Diabetes and Metabolism, Albert Einstein College of Medicine, Bronx, New York 10461 and the ^{||}Department of Medicine, Rutgers Robert Wood Johnson Medical School, New Brunswick, New Jersey 08901

Edited by Qi-Qun Tang

The Mediator complex plays a critical role in the regulation of transcription by linking transcription factors to RNA polymerase II. By examining mouse livers, we have found that in the fasted state, the Mediator complex exists primarily as an approximately 1.2-MDa complex, consistent with the size of the large Mediator complex, whereas following feeding, it converts to an approximately 600-kDa complex, consistent with the size of the core Mediator complex. This dynamic change is due to the dissociation and degradation of the kinase module that includes the MED13, MED12, cyclin-dependent kinase 8 (CDK8), and cyclin C (CCNC) subunits. The dissociation and degradation of the kinase module are dependent upon nutrient activation of mTORC1 that is necessary for the induction of lipogenic gene expression because pharmacological or genetic inhibition of mTORC1 in the fed state restores the kinase module. The degradation but not dissociation of the kinase module depends upon the E3 ligase, SCF^{FBW7}. In addition, genetically insulin-resistant and obese *db/db* mice in the fasted state displayed elevated lipogenic gene expression and loss of the kinase module that was reversed following mTORC1 inhibition. These data demonstrate that the assembly state of the Mediator complex undergoes physiologic regulation during normal cycles of fasting and feeding in the mouse liver. Furthermore, the assembly state of the Mediator complex is dysregulated in states of obesity and insulin resistance.

Gene transcription in eukaryotes is orchestrated through complex multistep processes that include chromatin reorganization coupled with transcription initiation, elongation, and termination, with the initiation being the most studied regulatory step in this process (1, 2). In the case of protein-encoding mRNA, the RNA polymerase II (Pol II)³ and the general

transcription factors, such as TFIIB, TFIID, TFIIE, TFIIF, and TFIH, constitute the basal transcription machinery (3, 4). The regulation of gene activation or repression engages specific sets of DNA-binding transcription factors. However, it is generally believed that the majority of transcription factors in eukaryotic cells do not directly interact with Pol II but instead engage a series of transcription cofactors, particularly the Mediator complex that interacts with multiple transcription factors and Pol II to integrate the transcriptional signals to the basal transcriptional machinery (5–7).

Biochemical isolation studies of the Mediator complex from cultured cancer cells have suggested the presence of at least two forms: the small or core Mediator complex composed of ~26 subunits with a size of ~600 kDa and the large Mediator complex that also contains the kinase module subunits (MED13, MED12, CDK8, and CCNC) but lacks the MED26 subunit with a size of ~1.2 MDa (8–11). Although some reports have suggested that the presence of multiple forms of the Mediator complex may be generated during the biochemical purification or due to the use of different cell lines (12, 13), other studies have reported that the small Mediator complex functions to activate transcription initiation, whereas the large Mediator complex is inactive or acts as a transcription repressor (14). In addition, the large Mediator complex has been linked to activation of transcription elongation (15), and the kinase module was found to function in a context-specific manner to either repress or activate transcription, depending on cell context, transcription factors, and/or target gene promoters (16–18). Recently, we reported that CDK8 and CCNC play an important role in the control of lipogenic gene expression through a nutrient-stimulated down-regulation in the liver (19). However, it is unclear whether the subunit assembly state of the whole Mediator complex is regulated under physiological or pathophysiological states.

In this study, we now demonstrate that the subunit assembly state of the Mediator complex in mouse liver undergoes dynamic normal physiologic regulation through a mTORC1-dependent down-regulation of the entire kinase module to generate the small Mediator complex. In addition, the degradation of the kinase module, but not its dissociation from the large Mediator complex, depends upon the E3 ligase SCF^{FBW7}.

This work was supported by National Institutes of Health Grants DK110063, DK098439, and DK020541. The authors declare that they have no conflicts of interest with the contents of this article. The content is solely the responsibility of the authors and does not necessarily represent the official views of the National Institutes of Health.

This article was selected as one of our Editors' Picks.

This article contains Table S1 and Figs. S1–S4.

¹ Supported by T32 postdoctoral training award AG023475.

² To whom correspondence should be addressed: Dept. of Medicine, Albert Einstein College of Medicine 375 Price Center, Bronx, NY 10461. Tel.: 718-678-1029; Fax: 718-678-1020; E-mail: Jeffrey.pessin@einstein.yu.edu.

³ The abbreviations used are: Pol II, RNA polymerase II; TBP, TATA-binding protein; MAP, mitogen-activated protein; qRT-PCR, real-time quantitative RT-PCR.

This is an open access article under the CC BY license.

9076 *J. Biol. Chem.* (2019) 294(23) 9076–9083



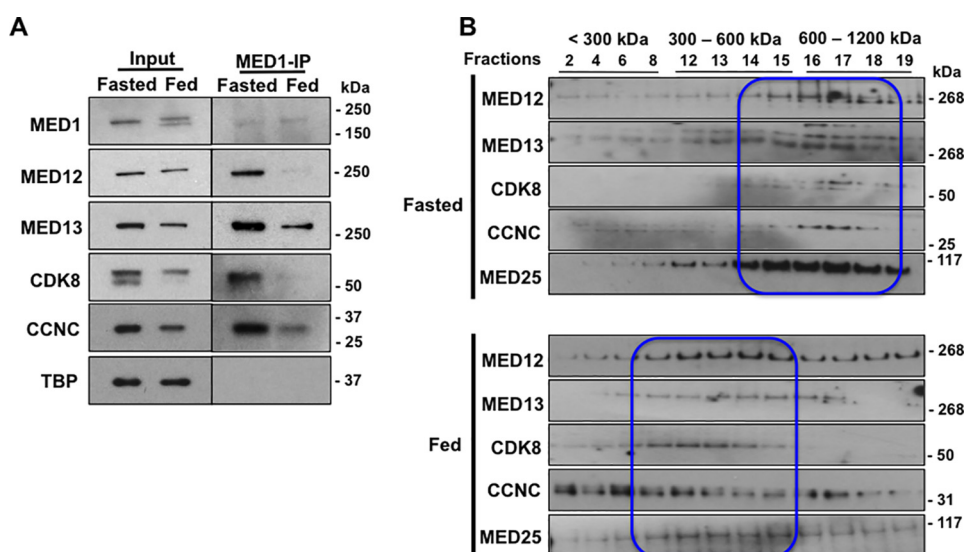


Figure 1. Dissociation of kinase module subunits upon nutrient signal is observed by immunoprecipitation. Ten-week-old male mice were subjected to the fasting and feeding protocol, and liver nuclear extractions were performed as described under "Experimental procedures" ($n = 6$ per group). *A*, representative MED1 immunoprecipitation (IP) and Western blot analysis of the Mediator subunits from pooled fasted or fed liver nuclear extracts. *B*, shift of various subunits to the size that correlates with different complexes shown on gels. Samples were obtained by glycerol gradient column separation with ultracentrifugation. Fractions 2–8 represent free subunits, fractions 12–15 represent small complexes, and fractions 16–19 represent large complexes according to the size standards.

Results

The kinase module is dissociated from the large Mediator complex and degraded upon nutrient signals

We have previously shown that the degradation of two subunits in the kinase module, CDK8, and its binding partner, CCNC, is triggered by nutrient signals in the liver (19). To determine whether other subunits of the Mediator complex are also regulated by nutrient availability, we compared the protein levels of additional subunits of the Mediator complex in the livers between mice that were fasted overnight and those that were fed for 4 h following the overnight fast. As observed previously, equal amounts of liver nuclear extracts (normalized for the nuclear TATA-binding protein (TBP)) displayed reduced levels of CKD8 and CCNC in the fed state (Fig. 1A). Similarly, there was also a reduction in MED13 and MED12 proteins with little effect on the levels of the Mediator subunit MED1. Immunoprecipitation with an antibody against MED1, which is present in both the small and large Mediator complexes (8–11), demonstrated a reduction in all four kinase module subunits that are associated with MED1 in the fed state (Fig. 1A), suggesting a shift from the large Mediator complex to the small Mediator complex upon feeding. To confirm the specificity of kinase module subunit antibodies, here we show the immunoblots of liver-specific *Ccnc* knockout mice that display the expected decrease in CDK8 and CCNC protein without significant effect on MED13 or MED12 protein levels (Fig. S1A). In contrast, liver-specific knockout of *Med13* knockout results in decreased protein levels of all four kinase module proteins MED13, MED12, CCNC, and CDK8 (Fig. S1B).

The reduction in the protein levels of the kinase module subunits occurred without any significant change in the amounts of mRNAs encoding for the Mediator subunits (Fig. S2). To further confirm this apparent change in the Mediator subunit

assembly state, we examined the size distribution of the Mediator complex by glycerol gradient fractionation. Based on the molecular size standards, the small Mediator complex (~600 kDa) should be in fractions 12–15, whereas the large Mediator complex (~1.2 MDa) should be in fractions 16–19 (Fig. 1B). In fasted state, it was apparent that all of the subunits were in the large Mediator form, as both the core subunit (MED25) and kinase module subunits were enriched in the later fractions that match with the size of the large Mediator complex (~1.2 MDa) (Fig. 1B). In contrast, the enrichment of all subunits was shifted to the left with the major distribution located in fractions 12–15 in the fed livers to the size close to the small Mediator complex or the kinase module alone (Fig. 1B). It is also important to note that the glycerol gradient fractionation analyses do not reflect the relative amounts of proteins present between fasting and feeding, but only the relative sizes of protein complexes that they are associated with, as greater amounts of nuclear extracts from fed livers were used, and the gel exposures were not identical in order to observe the less abundant kinase module subunits.

The nutrient-sensitive mTORC1 signaling pathway is responsible for the degradation and dissociation of the kinase module

To explore the role of mTORC1 signaling in the regulation of protein levels of the kinase module subunits, we first took a pharmacological approach by using the mTORC1-specific inhibitor rapamycin. Mice were fasted, fed, or treated with rapamycin before induction of the fed state. As observed by others, rapamycin effectively blocked the feeding-induced activation of mTORC1 kinase activity, as demonstrated by the inhibition of S6K1 and S6 phosphorylation (Fig. 2A). In addition, rapamycin blocked the induction of lipogenic gene expression in the fed state but has no significant effect on glucone-

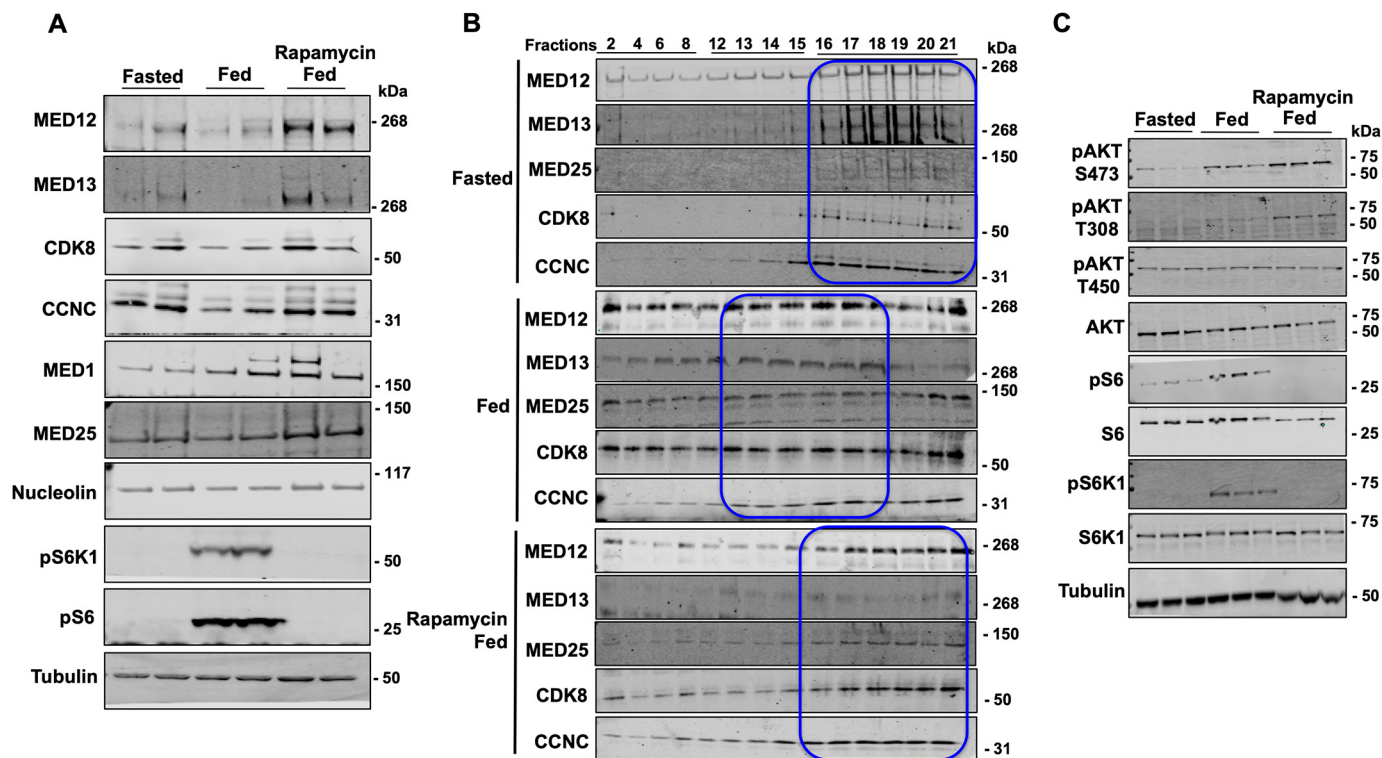


Figure 2. Kinase module subunits are degraded and dissociated from the core complex upon nutrient signal through mTORC1-dependent pathway. Twelve-week-old male mice were injected with vehicle or 1 mg/kg rapamycin every 6 h over 2 days period and then subjected to the fasting and feeding protocol as described under "Experimental procedures" ($n = 6$ per group). *A*, Western blot analysis of the kinase module subunits as well as the core module subunit MED25 from two independent isolated liver nuclear extracts. *B*, shift of various subunits to the size that correlates with different complexes shown on gels. Samples were obtained by glycerol gradient column separation with ultracentrifugation. Fractions 2–8 represent free subunits, fractions 12–15 represent small complexes, and fractions 16–21 represent large complexes according to the size standards. *C*, Western blotting was performed from total liver tissue extracts.

genic gene expression levels (Fig. S3, *A* and *B*). In concert, the reduction in the kinase module subunits MED12, MED13, CDK8, and CCNC in the fed state was prevented when the mice were pretreated with rapamycin (Fig. 2*A*). To determine whether mTORC1 inhibition also prevents the feeding-induced formation of the small Mediator complex, we analyzed the liver nuclear extracts by glycerol gradient fractionation. Consistent with the data in Fig. 1, in the fasted state, the Mediator complex primarily resolved as the large Mediator complex (centered around \sim 1.2 MDa), whereas in the fed state, it shifted to a smaller size consistent with the small Mediator complex (Fig. 2*B*). However, feeding of the rapamycin-treated mice prevented the formation of the small Mediator complex, as the Mediator complex mostly fractionated in the position of the large Mediator complex (Fig. 2*B*). The specificity of rapamycin for mTORC1 was verified by examining the phosphorylation of AKT, in which both Ser-473 and Thr-450 are thought to be mTORC2 target sites (20, 21). As expected, the phosphorylation of Thr-450 was unaffected by rapamycin, and both Ser-473 and Thr-308 were found to be further increased in the fed state following rapamycin pretreatment (Fig. 2*C*). These data confirm the specificity of rapamycin for mTORC1 and are also consistent with mTORC1 activation acting in a feedback pathway to reduce AKT activation (22).

To further examine the role of mTORC1 in the regulation of the Mediator complex, we generated hepatocyte-specific *Raptor* knockout mice via injecting AAV8-Tbg-Cre in the tail vein

of *Raptor*^{f/f} mice. RAPTOR is a critical component of mTORC1, and knockout of *Raptor* completely abolishes the mTORC1 pathway but not mTORC2 (23, 24). These liver-specific *Raptor* knockout mice displayed a marked reduction of the S6K1 phosphorylation consistent with reduced mTORC1 activation along with prevention of the loss of the kinase module proteins in the fed state (Fig. 3*A*). Although *Raptor* deficiency did not affect the suppression of gluconeogenic genes in the fed state (Fig. 3*B*), there was a substantial reduction of lipogenic gene expression (Fig. 3*C*). In parallel, *Raptor* deficiency also blocked the conversion of the large Mediator complex to the small Mediator complex in the fed state (Fig. 3*D*).

The effect of loss of function of mTORC1 activity by rapamycin and *Raptor* deficiency was further confirmed by analyses of mTORC1 gain of function using liver-specific *Tsc1* knockout mice, in which the mTORC1 pathway is constitutively active. The constitutive activation of mTORC1 was confirmed by the increased levels of S6K1 phosphorylation in both the fasted and fed state in the *Tsc1* knockout liver hepatocytes. As observed previously, control mice in the fed state had reduced MED13, MED12, CDK8, and CCNC protein levels compared with those in the fasted state (Fig. S4). In contrast, following *Tsc1* deletion, the levels of these proteins were relatively low in the fasted state and refractory to any further change following feeding (Fig. S4).

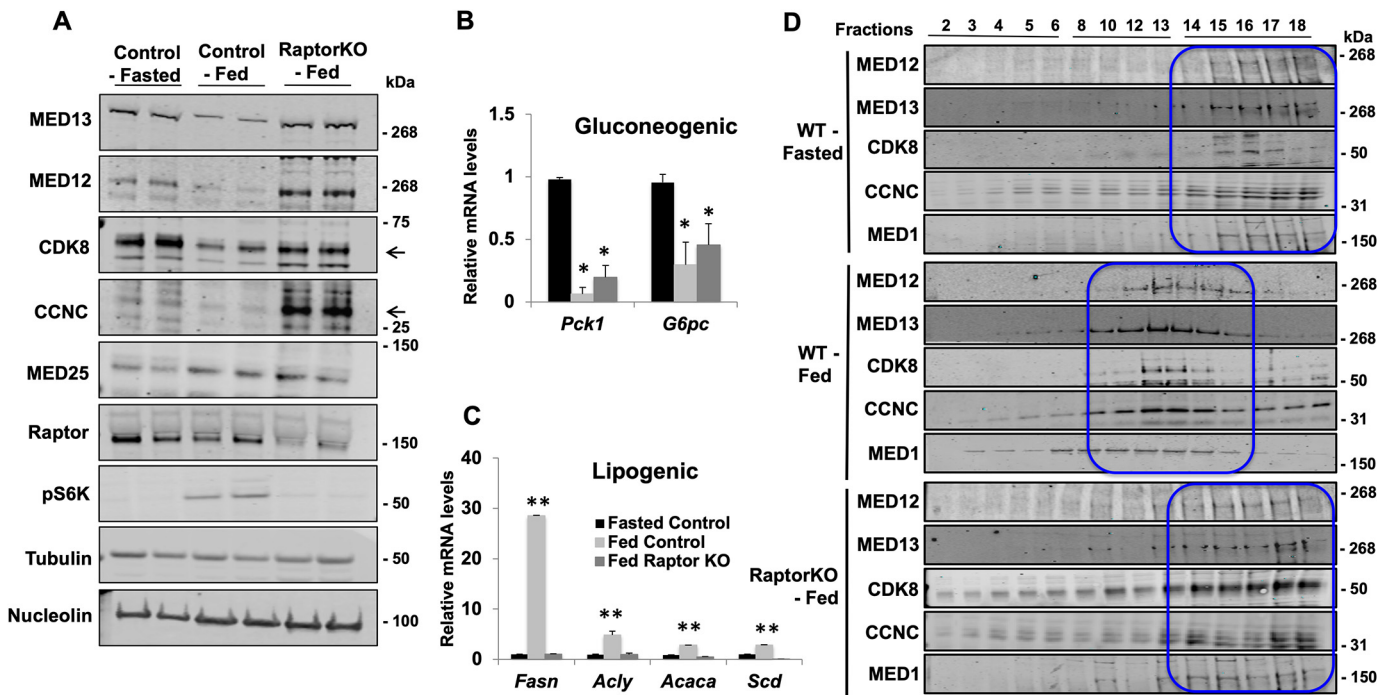


Figure 3. Inhibition of mTORC1 pathway protects kinase module from degradation and dissociation. Twelve-week-old *Raptor*^{f/f} mice were tail vein-injected with either AAV8-Tbg-eGFP (Control) or AAV8-Tbg-Cre (Raptor knockout) and fed *ad libitum* for 10 days. The control and *Raptor* knockout mice were subjected to the fasting and feeding protocol described under "Experimental procedures" ($n = 6$ per group). *A*, Western blot analysis of the Mediator subunits and cytosolic kinases from two independent isolated liver nuclear extracts are shown. *B* and *C*, real-time quantitative RT-PCR (qRT-PCR) of genes involved in gluconeogenesis (*Pck1* and *G6pc*) and lipogenesis (*Fasn*, *Scd1*, *Acaca*, and *Acly*) in livers of fasted, fed, or liver-specific *Raptor* knockout fed mice. *p* values were obtained by Student's *t* test. *, $p < 0.05$ versus fasted liver; **, $p < 0.05$ versus all others. Values are the mean \pm S.E. (error bars). *D*, shift of various subunits to the size that correlates with different complex sizes shown on gels. Samples were obtained by glycerol gradient column separation with ultracentrifugation. Fractions 2–6 represent free subunits, fractions 8–13 represent small complexes, and fractions 14–18 represent large complexes according to size standards.

Degradation and dissociation of the kinase module subunits are increased in insulin-resistant and obese mice

Previously, we reported that the livers of the insulin-resistant and obese *db/db* mice display elevated mTORC1 activation in the fasted state, and this was confirmed in Fig. 4*A*. Consistent with this fasted state activation of mTORC1, the Mediator kinase module subunits were reduced compared with the fasted control mice. Importantly, treatment with rapamycin to suppress mTORC1 activation resulted in a concomitant rescue of the kinase module proteins (Fig. 4*A*), suggesting that mTORC1 is the major driver for the loss of the kinase module. As expected, rapamycin treatment of the *db/db* mice also suppressed the abnormal elevation of lipogenic gene expression in the fasted state (Fig. 4*B*) with little effect on the key gluconeogenic gene *Pck1* (Fig. 4*C*) but with a small reduction of *G6pc* mRNA by ~50%. In any case, glycerol gradient fractionation demonstrated a large shift to smaller sizes of the Mediator complex in the fasted *db/db* mice livers compared with control mice, and the complex was mostly reversed back to the large Mediator complex following rapamycin treatment (Fig. 4*D*).

Dissociation of the kinase module from the large Mediator complex is not dependent on protein degradation

Next, we examined whether blocking the degradation of the kinase module is sufficient to prevent the feeding-induced formation of the small Mediator complex. *In vitro* studies have suggested that the E3 ubiquitin ligase component FBW7 can induce the degradation of MED13 (25), which links the kinase

module to the core Mediator complex (14, 26, 27). We therefore tested whether FBW7 is necessary for the degradation and/or dissociation of the kinase module *in vivo* using acute hepatocyte-specific *Fbw7* knockout mice generated by tail vein injection of AAV8-Tbg-Cre into *Fbw7*^{f/f} mice. Control mice in the fed state displayed the typical decrease in the Mediator kinase module subunits that was prevented in the hepatocyte-specific *Fbw7*-deficient mice (Fig. 5*A*). Consistent with functioning downstream of mTORC1, *Fbw7* deficiency had no significant effect on the activation of mTORC1 kinase activity in the fed state (Fig. 5*B*). Interestingly, despite the restoration of the kinase module proteins in the *Fbw7* knockout livers, the Mediator complex is still converted to the small Mediator and the kinase module complexes following feeding (Fig. 5*E*), indicating that stabilizing the kinase module subunits is not sufficient to block the feeding-induced dissociation of this module from the large Mediator complex. In parallel, both the control and *Fbw7* knockout livers displayed elevated gluconeogenic genes in the fasted state that was suppressed in the fed state, whereas the lipogenic genes were increased in the fed state and suppressed in the fasted state (Fig. 5, *C* and *D*). Although the relative changes in *Pck1* and *Fasn* were not significantly different between control and *Fbw7* knockout livers, we have consistently observed that the fasting-induced expression of *G6pc* was reduced, whereas the feeding-induced expression of *Acly*, *Acaca*, and *Scd1* were enhanced in the liver-specific *Fbw7* knockout mice.

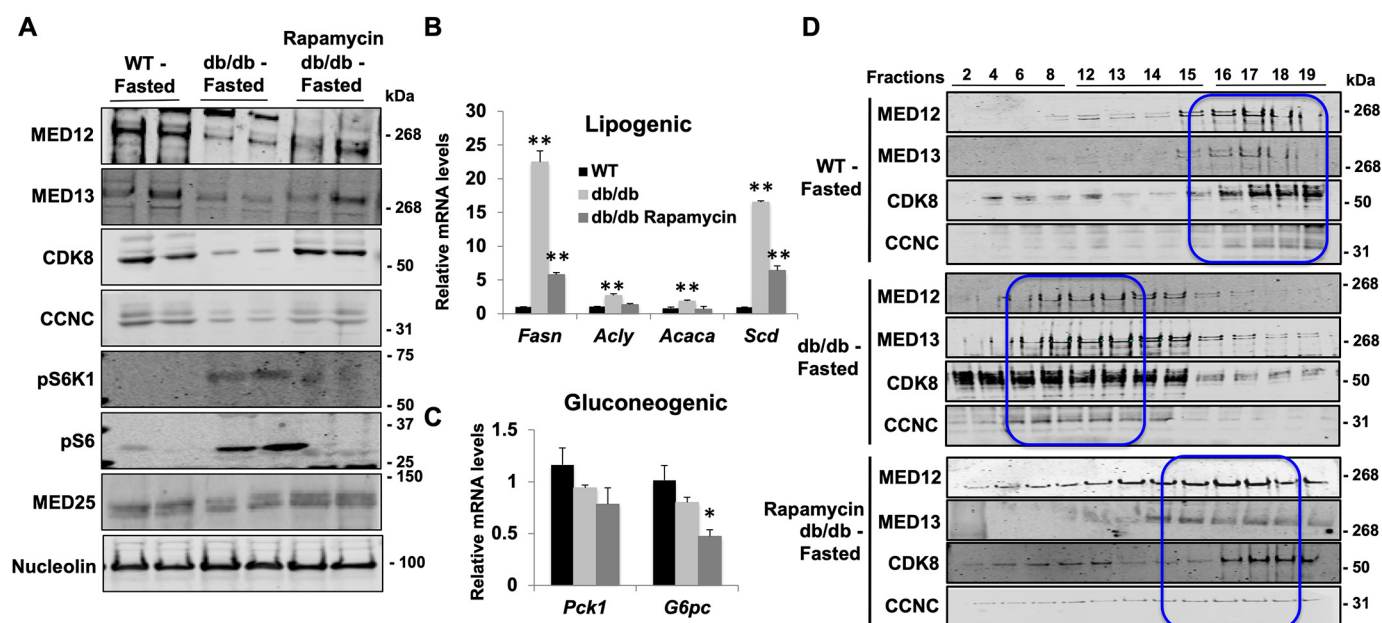


Figure 4. Changes in the Mediator complex kinase subunits protein levels and assembly state in db/db mice. Twelve-week-old WT C57BL/6J and db/db male mice on a C57BL/6J background were injected with vehicle or 1 mg/kg rapamycin every 6 h over a 2-day period and then fasted as described under "Experimental procedures" ($n = 4$ per group). A, Western blot analysis of the Mediator subunits and cytosolic kinases from two independent isolated liver nuclear extracts are shown. B and C, qRT-PCR of genes involved in lipogenesis (*Fasn*, *Scd1*, *Acaca*, and *Acyl*) and gluconeogenesis (*Pck1* and *G6pc*) in livers of fasted WT or db/db mice treated with either vehicle or rapamycin. p values were obtained by Student's *t* test. *, $p < 0.05$ versus WT; **, $p < 0.05$ versus all others. Values are the mean \pm S.E. (error bars). D, shift of various subunits to the size that correlates with different complexes shown on gels. Samples were obtained by glycerol gradient column separation with ultracentrifugation. Fractions 2–8 represent free subunits, fractions 12–15 represent small complexes, and fractions 16–19 represent large complexes according to the size standards.

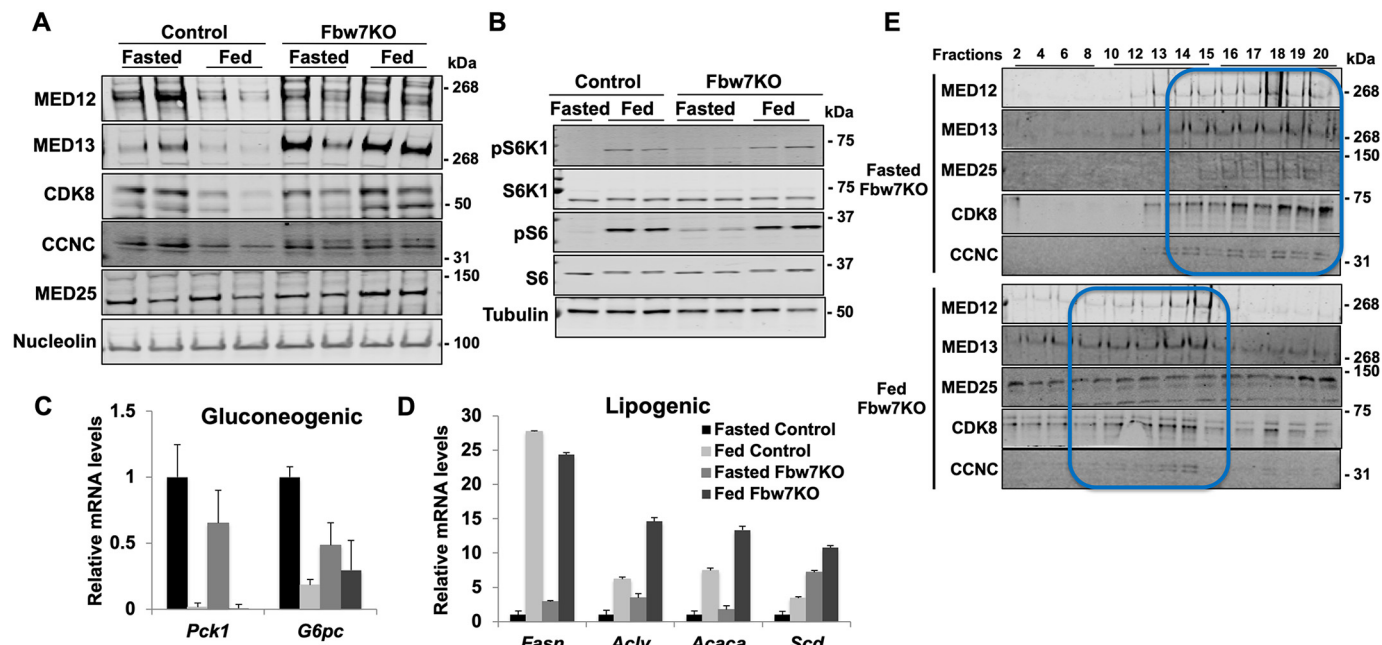


Figure 5. SCF^{FBW7} promotes MED13 degradation but not responsible for the dissociation of kinase module. Nine-week-old *Fbw7*^{f/f} male mice were either untreated (Control) or tail vein-injected with AAV8-Tbg-Cre (*Fbw7KO*) to generate acute liver-specific knockout mice. Ten days following injection, the knockout and control mice were subjected to the fasting and feeding protocol described under "Experimental procedures" ($n = 8$ per group). A and B, Western blot analysis of the Mediator subunits and cytosolic kinases from two independent isolated liver nuclear extracts are shown. C and D, qRT-PCR of genes involved in lipogenesis (*Fasn*, *Scd1*, *Acaca*, and *Acyl*) and gluconeogenesis (*Pck1* and *G6pc*) in livers of fasted and fed WT mice ($n = 6$ per group). E, kinase subunits and MED25 from the core complex were detected by Western blot analysis after glycerol gradient column size separation. Fractions 2–8 represent complexes that match with the sizes of free subunits, fractions 10–15 represent small complexes, and fractions 16–20 represent large complexes according to the size standards. Error bars, S.E.

Discussion

The Mediator complex is a multisubunit protein complex that directly binds to multiple DNA sequence-specific tran-

scription factors (28–31). The Mediator complex simultaneously engages Pol II and thereby integrates and conveys gene-specific regulation for transcription initiation and/or

elongation (28, 30). Biochemical analyses of the Mediator complex have identified at least two major complexes in cultured cancer cells, the large Mediator complex and the small/core Mediator (11). Previous studies have suggested that the small Mediator complex functions primarily in transcriptional initiation, whereas the large Mediator complex participates in transcription elongation (11, 14, 15). Mutational analyses have further shown that the *Saccharomyces cerevisiae* also has an equivalent of the mammalian small Mediator to activate Pol II-dependent transcription initiation (16). It has been assumed that the large and small Mediator complexes exist as two static complexes in cells that control different subsets of regulated gene expression. Although recent studies have shown that CDK8 and CCNC protein levels are regulated under various nutritional states in the *Drosophila* fat body and mouse liver (19, 32), whether this reflects Mediator complex-associated or free CDK8/CCNC subunits was not examined. In yeast, oxidative stress has also been reported to induce nuclear CCNC export and degradation of MED13 (33), but whether this occurs under normal physiologic conditions or in mammalian cells was not assessed.

Our study of mouse liver revealed a dynamic oscillation of different forms of the Mediator complexes between fasting and feeding. Based on molecular weights, our data demonstrate that the hepatic Mediator complex primarily exists in the form of the large Mediator complex in the fasted state. However, following feeding, the kinase module (MED13/MED12/CDK8/CCNC) undergoes dissociation and degradation, resulting in the formation of the small Mediator complex. Although it is currently unclear whether there are any changes in the small Mediator complex upon feeding, our data suggest that the previous identification of different Mediator complexes is not biochemical artifacts but exists due to the presence of different signals. In yeast, peroxide-induced degradation of MED13 is promoted via MAP kinase SIT2/MPK1 and the AMP-dependent protein kinase SNF1-dependent manner (34). However, using both pharmacological and genetic inhibition, we clearly demonstrate that the feeding-induced activation of mTORC1, but not mTORC2, is necessary for the dissociation of the kinase module correlated with the activation of lipogenic gene expression in mouse livers. mTORC1 is an important target of numerous signaling pathways and serves as a critical sensor of nutrient status. Our data provide compelling evidence that mTORC1 activation is sufficient for the nutrient-dependent dissociation and degradation of the liver Mediator kinase module *in vivo*. However, whether mTORC1 activation *per se* is sufficient for activation of lipogenic gene expression is still an open question; this also requires the activation of a variety of DNA-binding transcription factors and co-regulators.

Despite this caveat, hyperphagic, obese, and insulin-resistant *db/db* mice display elevated mTORC1 activity in the fasted state along with the down-regulation of the kinase module, formation of the small Mediator complex, and enhanced lipogenic gene expression. Rapamycin inhibition of mTORC1 resulted in increased kinase module protein levels, reassembly of the large Mediator complex, and suppression of lipogenic gene expression, whereas constitutive activation of mTORC1 resulted in decreased kinase module proteins, consistent with formation of

the small Mediator complex. These data clearly demonstrate that from the perspective of the Mediator complex, fasted *db/db* mice appear to be in the fed state due to the basal activation of mTORC1.

The SCF^{FBW7} E3 ligase ubiquitinates target proteins that are phosphorylated at a conserved phosphodegron motif, $\Phi\chi\Phi\Phi(T/S)PPX(T/S/E/D)$ (25). In human embryo kidney HEK293 cells, co-expression of MED13 with the SCF^{FBW7} E3 ligase was shown to induce the degradation of the MED13 protein, and mutation of Ser-323 or Ser-326 reduced FBW7-mediated degradation (25). In agreement with these cell culture results, using liver-specific *Fbw7* knockout mice, we also found that the degradation of the kinase module depends on SCF^{FBW7}. However, despite the stabilization of the kinase module, the Mediator complex is still converted to the small Mediator complex in the fed state. These data indicate that FBW7 is necessary for the degradation of the kinase module but is independent of the mTORC1-dependent signals required for the dissociation of the kinase module from the large Mediator complex. The SCF^{FBW7} phosphodegron motif is present in a number of important regulatory proteins, including SREBP-1c, and is required for the termination of lipogenic gene expression by mediating the degradation of nuclear SREBP-1c protein (35). This also accounts for the small increase in both basal and nutrient-stimulated lipogenic gene expression in the liver-specific *Fbw7* knockout mice.

Although we have yet to identify the specific kinase(s)/phosphatase(s) regulating the phosphorylation of the MED13 phosphodegron motif, it is unlikely that either of the identified mammalian orthologs of the yeast kinases is responsible. In the fed state, the mammalian ortholog of SNF1, the AMP-dependent protein kinase, is inactive in mouse liver. Although MAP kinases can be activated in the fed state, the MED13 phosphodegron motif is not a consensus sequence for the mammalian family of MAP kinase (34). It is also less likely that mTORC1 is the direct kinase responsible as mTORC1 is primarily thought to be active at the lysosome (36), and evidence for nuclear localization has yet to be compelling. Alternatively, certain subunits in the small Mediator complex may also be post-translationally modified upon feeding, resulting in conformational changes of the Mediator complex so that the kinase module may be dissociated from the large Mediator complex. Future work will identify these molecular details. Nevertheless, our study shows for the first time that the assembly state of the Mediator complex is dynamically regulated at least in the liver under physiological and pathophysiological conditions, and the mTORC1 signaling is the major upstream regulator of the Mediator complex *in vivo*.

Experimental procedures

Animals

All animal experiments followed the guidelines that were approved and in agreement with the Albert Einstein College of Medicine Institutional Animal Care and Use Committee (2016-0901). C57B6/J, *Raptor*^{fl/fl}, *Fbw7*^{fl/fl}, *Tsc1*^{fl/fl}, and *db/db* mice in C57BLKS/J background were obtained from the Jackson Laboratory. *Ccnc*^{fl/fl} mice were obtained as described previously

(37), and *Med13^{f/f}* mice were kindly provided by Dr. Eric Olson. AAV8-Tbg-Cre (Vector Biolabs) was introduced by intravenous injection at 5×10^{11} genome copies/mouse to generate the respective liver-specific knockout mice. For rapamycin studies, 1 mg/kg body weight of rapamycin (LC Laboratories) was injected every 6 h over a 48-h period. Mice were housed in groups and in a facility equipped with a 12-h light/dark cycle with free access to food and water and were fed with a normal chow diet unless noted otherwise.

Mice were provided standard laboratory mouse chow (Lab-Diet catalog no. 5053) that contains 25% protein, 13% fat, and 62% carbohydrates. For fasting and feeding experiments, mice were trained for 3 days before the experiment by removing food at 5 p.m. and feeding at 9 a.m. the next day (16-h fast overnight and 8-h feeding daytime). On day 4, the fasting group of mice was sacrificed in the morning at 11 a.m. (18-h fast), whereas the 9 a.m. fed group was also provided drinking water that contained 15% sucrose (w/v). The fed mice were sacrificed at 1 p.m., equal to 4 h of feeding.

Antibodies and immunoblotting

Antibodies against the following proteins were used in this study: MED13 (Fisher PA5-35924 (1:1000) or Bethyl A301-278A (1:1000)), MED12 (Abcam ab70842 (1:1000)), CDK8 (Abcam ab54561 (1:1000) or Bethyl A302-501A-M (1:1000)), CCNC (Bethyl A301-989A (1:1000)), MED1 (Bethyl A300-793A (1:1000)), MED25 (Fisher PA5-43616 (1:1000)), MED15 (Bethyl A302-422A (1:1000)), nucleolin (Cell Signaling 14574S (1:1000)), tubulin (Cell Signaling 2144S (1:1000)), phospho-p70 S6 kinase (Cell Signaling 9234S (1:1000)), p70 S6 kinase (Cell Signaling 2708T (1:1000)), phospho-S6 ribosomal protein (Cell Signaling 4858P (1:1000)), S6 ribosomal protein (Cell Signaling 2317S (1:1000)), TBP (Cell Signaling 8515S (1:1000)), phospho-AKT Ser-473 (Cell Signaling 4060 (1:1000)), Thr-308 (Cell Signaling 4056 (1:1000)), Thr-450 (Cell Signaling 12178 (1:1000)), total AKT (Cell Signaling 9272 (1:1000)), and RAPTOR (Cell Signaling 2280 (1:1000)). Total liver tissue lysates were prepared using the Pierce IP lysis buffer (87787, Thermo Fisher Scientific) with freshly added 1 mM DTT, protease inhibitors, and phosphatase inhibitors. Protein samples were loaded onto 3–8% Tris acetate gels (Invitrogen) and transferred to nitrocellulose membrane (Invitrogen, iBlot gel transfer). Western blotting signals were detected with either goat anti-rabbit or goat anti-mouse secondary antibodies (IRDye 800CW) from LI-COR.

RNA isolation and quantitative PCR

Total RNA isolation from mouse livers and quantitative PCR analysis were performed as described previously (19). For RNA purification, the RNeasy purification kit (Qiagen) was used according to the manufacturer's protocol. The first-strand cDNA was synthesized by using the SuperScript VILO cDNA synthesis kit (Invitrogen). The PowerUp SYBR Green Master Mix (Applied Biosystems) was used for quantitative PCR and quantitated using the StepOnePlus real-time PCR system (Applied Biosystems). Samples were normalized to the *Ppib* gene to determine relative mRNA levels. The primer sequences used in this study are listed in Table S1.

Nuclear extraction and glycerol gradient fractionation

Fresh mouse liver nuclear extracts were prepared as described previously with some modifications (38). A mixture of protease inhibitors (Sigma-Aldrich), phosphatase inhibitors (Sigma-Aldrich), and 1 mM DTT was added to all buffers immediately before use, and all procedures were performed on ice in a 4 °C cold room. The pooled liver extracts for each condition were then loaded directly onto a glycerol gradient column generated by an automix gradient former (Jule, Inc.) with 40 and 80% (w/v) glycerol in gradient buffer (20 mM Hepes, 100 mM NaCl, 1.5 mM MgCl₂, pH 7.8) on top of a 200-μl cushion of 100% glycerol. Gradients containing samples or native marker protein standards that ran in parallel (Invitrogen) were centrifuged at 16,000 × g for 16 h at 4 °C in a Beckman ultracentrifuge with SW55 Ti or VTi 65.2 rotors. Gradient fractions (50–100 μl) were collected from the top of the column and analyzed by Western blotting. Fractions taken from the protein standard column were resolved on NuPAGE 3–8% Tris acetate native gel (Thermo Fisher Scientific) followed by silver staining and compared with the fractions from the lysate samples.

Immunoprecipitation

Fresh mouse liver nuclei were isolated as described previously with some modifications (38). Mouse liver nuclear were incubated in extraction buffer A containing 20 mM Tris-HCl, pH 8.0, 420 mM NaCl, 1.5 mM MgCl₂, 0.2 mM EDTA, 20% glycerol, 12% sucrose, 1 mM DTT, 2.5 mM phenylmethylsulfonyl fluoride, 1 mM benzamidine, and 1 mg/liter aprotinin. The nuclear extracts were then dialyzed against 500 volumes of buffer D (20 mM Tris-HCl, pH 8.0, 100 mM KCl, 1.5 mM MgCl₂, 0.1 mM EDTA, 20% glycerol, 1 mM DTT, 2.5 mM phenylmethylsulfonyl fluoride, and 1 mM benzamidine). After centrifugation at 20,000 × g for 20 min at 4 °C, the resulting supernatants were used for immunoprecipitation. Ten microliters of anti-MED1 antibody was bound to 20 μl of protein A/G beads (Pharmacia) for 30 min at room temperature and incubated with 200 μl of liver nuclear extracts for 3 h at 4 °C. The beads were washed five times with 1 ml of buffer containing 0.1% Nonidet P-40. Interacting proteins were eluted with buffer containing 0.3% Sarkosyl.

Statistical analysis

Data are presented as the mean ± S.E. unless otherwise noted and compared between two groups using Student's *t* test. A two-sided *p* < 0.05 was considered statistically significant.

Author contributions—D. Y. Y., F. Y., and J. E. P. conceptualization; D. Y. Y., A. M. X., and H. K. data curation; D. Y. Y. formal analysis; D. Y. Y. validation; D. Y. Y. investigation; D. Y. Y. visualization; D. Y. Y. and A. M. X. methodology; D. Y. Y. writing-original draft; F. Y. and J. E. P. resources; F. Y. and J. E. P. supervision; F. Y. and J. E. P. funding acquisition; F. Y. and J. E. P. writing-review and editing; J. E. P. project administration.

References

1. Sauer, F., and Tjian, R. (1997) Mechanisms of transcriptional activation: differences and similarities between yeast, *Drosophila*, and man. *Curr. Opin. Genet. Dev.* 7, 176–181 CrossRef Medline

2. Nogales, E., Louder, R. K., and He, Y. (2017) Structural Insights into the Eukaryotic Transcription Initiation Machinery. *Annu. Rev. Biophys.* **46**, 59–83 [CrossRef](#) [Medline](#)
3. Hahn, S. (2004) Structure and mechanism of the RNA polymerase II transcription machinery. *Nat. Struct. Mol. Biol.* **11**, 394–403 [CrossRef](#) [Medline](#)
4. Thomas, M. C., and Chiang, C. M. (2006) The general transcription machinery and general cofactors. *Crit. Rev. Biochem. Mol. Biol.* **41**, 105–178 [CrossRef](#) [Medline](#)
5. Thompson, C. M., Koleske, A. J., Chao, D. M., and Young, R. A. (1993) A multisubunit complex associated with the RNA polymerase II CTD and TATA-binding protein in yeast. *Cell* **73**, 1361–1375 [CrossRef](#) [Medline](#)
6. Kim, Y. J., Björklund, S., Li, Y., Sayre, M. H., and Kornberg, R. D. (1994) A multiprotein mediator of transcriptional activation and its interaction with the C-terminal repeat domain of RNA polymerase II. *Cell* **77**, 599–608 [CrossRef](#) [Medline](#)
7. Takagi, Y., and Kornberg, R. D. (2006) Mediator as a general transcription factor. *J. Biol. Chem.* **281**, 80–89 [CrossRef](#) [Medline](#)
8. Dotson M. R., Yuan, C. X., Roeder, R. G., Myers, L. C., Gustafsson, C. M., Jiang, Y. W., Li, Y., Kornberg, R. D., and Asturias, F. J. (2000) Structural organization of yeast and mammalian mediator complexes. *Proc. Natl. Acad. Sci. U.S.A.* **97**, 14307–14310 [CrossRef](#) [Medline](#)
9. Liu, Y., Ranish, J. A., Aebersold, R., and Hahn, S. (2001) Yeast nuclear extract contains two major forms of RNA polymerase II mediator complexes. *J. Biol. Chem.* **276**, 7169–7175 [CrossRef](#) [Medline](#)
10. Malik, S., Baek, H. J., Wu, W., and Roeder, R. G. (2005) Structural and functional characterization of PC2 and RNA polymerase II-associated subpopulations of metazoan Mediator. *Mol. Cell. Biol.* **25**, 2117–2129 [CrossRef](#) [Medline](#)
11. Taatjes, D. J., Näär, A. M., Andel, F., 3rd, Nogales, E., and Tjian, R. (2002) Structure, function, and activator-induced conformations of the CRSP coactivator. *Science* **295**, 1058–1062 [CrossRef](#) [Medline](#)
12. Wang, G., Cantin, G. T., Stevens, J. L., and Berk, A. J. (2001) Characterization of mediator complexes from HeLa cell nuclear extract. *Mol. Cell. Biol.* **21**, 4604–4613 [CrossRef](#) [Medline](#)
13. Sato, S., Tomomori-Sato, C., Parmely, T. J., Florens, L., Zybalov, B., Swanson, S. K., Banks, C. A., Jin, J., Cai, Y., Washburn, M. P., Conaway, J. W., and Conaway, R. C. (2004) A set of consensus mammalian mediator subunits identified by multidimensional protein identification technology. *Mol. Cell* **14**, 685–691 [CrossRef](#) [Medline](#)
14. Tsai, K. L., Sato, S., Tomomori-Sato, C., Conaway, R. C., Conaway, J. W., and Asturias, F. J. (2013) A conserved Mediator-CDK8 kinase module association regulates Mediator-RNA polymerase II interaction. *Nat. Struct. Mol. Biol.* **20**, 611–619 [CrossRef](#) [Medline](#)
15. Donner, A. J., Ebmeier, C. C., Taatjes, D. J., and Espinosa, J. M. (2010) CDK8 is a positive regulator of transcriptional elongation within the serum response network. *Nat. Struct. Mol. Biol.* **17**, 194–201 [CrossRef](#) [Medline](#)
16. Nemet, J., Jelicic, B., Rubelj, I., and Sopta, M. (2014) The two faces of Cdk8, a positive/negative regulator of transcription. *Biochimie* **97**, 22–27 [CrossRef](#) [Medline](#)
17. Mo, X., Kowenz-Leutz, E., Xu, H., and Leutz, A. (2004) Ras induces mediator complex exchange on C/EBP β . *Mol. Cell* **13**, 241–250 [CrossRef](#) [Medline](#)
18. Liu, Y., Kung, C., Fishburn, J., Ansari, A. Z., Shokat, K. M., and Hahn, S. (2004) Two cyclin-dependent kinases promote RNA polymerase II transcription and formation of the scaffold complex. *Mol. Cell. Biol.* **24**, 1721–1735 [CrossRef](#) [Medline](#)
19. Feng, D., Youn, D. Y., Zhao, X., Gao, Y., Quinn, W. J., 3rd, Xiaoli, A. M., Sun, Y., Birnbaum, M. J., Pessin, J. E., and Yang, F. (2015) mTORC1 down-regulates cyclin-dependent kinase 8 (CDK8) and cyclin C (CycC). *PLoS One* **10**, e0126240 [CrossRef](#) [Medline](#)
20. Sarbassov, D. D., Guertin, D. A., Ali, S. M., and Sabatini, D. M. (2005) Phosphorylation and regulation of Akt/PKB by the rictor-mTOR complex. *Science* **307**, 1098–1101 [CrossRef](#) [Medline](#)
21. Facchinetto, V., Ouyang, W., Wei, H., Soto, N., Lazorchak, A., Gould, C., Lowry, C., Newton, A. C., Mao, Y., Miao, R. Q., Sessa, W. C., Qin, J., Zhang, P., Su, B., and Jacinto, E. (2008) The mammalian target of rapamycin complex 2 controls folding and stability of Akt and protein kinase C. *EMBO J.* **27**, 1932–1943 [CrossRef](#) [Medline](#)
22. Manning, B. D. (2004) Balancing Akt with S6K: implications for both metabolic diseases and tumorigenesis. *J. Cell Biol.* **167**, 399–403 [CrossRef](#) [Medline](#)
23. Guertin, D. A., Stevens, D. M., Thoreen, C. C., Burds, A. A., Kalaany, N. Y., Moffat, J., Brown, M., Fitzgerald, K. J., Sabatini, D. M. (2006) Ablation in mice of the mTORC components raptor, rictor, or mLST8 reveals that mTORC2 is required for signaling to Akt-FOXP and PKC α but not S6K1. *Dev. Cell* **11**, 859–871 [CrossRef](#) [Medline](#)
24. Bentzinger, C. F., Romanino, K., Cloëtta, D., Lin, S., Mascarenhas, J. B., Oliveri, F., Xia, J., Casanova, E., Costa, C. F., Brink, M., Zorzato, F., Hall, M. N., and Rüegg, M. A. (2008) Skeletal muscle-specific ablation of raptor, but not of rictor, causes metabolic changes and results in muscle dystrophy. *Cell Metab.* **8**, 411–424 [CrossRef](#) [Medline](#)
25. Davis, M. A., Larimore, E. A., Fissel, B. M., Swanger, J., Taatjes, D. J., and Clurman, B. E. (2013) The SCF-Fbw7 ubiquitin ligase degrades MED13 and MED13L and regulates CDK8 module association with Mediator. *Genes Dev.* **27**, 151–156 [CrossRef](#) [Medline](#)
26. Knuesel, M. T., Meyer, K. D., Bernecky, C., and Taatjes, D. J. (2009) The human CDK8 subcomplex is a molecular switch that controls Mediator coactivator function. *Genes Dev.* **23**, 439–451 [CrossRef](#) [Medline](#)
27. Kuuluvainen, E., Hakala, H., Havula, E., Sahal Estimé, M., Rämet, M., Hiitakangas, V., and Mäkelä, T. P. (2014) Cyclin-dependent kinase 8 module expression profiling reveals requirement of mediator subunits 12 and 13 for transcription of Serpent-dependent innate immunity genes in *Drosophila*. *J. Biol. Chem.* **289**, 16252–16261 [CrossRef](#) [Medline](#)
28. Malik, S., and Roeder, R. G. (2010) The metazoan Mediator co-activator complex as an integrative hub for transcriptional regulation. *Nat. Rev. Genet.* **11**, 761–772 [CrossRef](#) [Medline](#)
29. Conaway, R. C., and Conaway, J. W. (2011) Origins and activity of the Mediator complex. *Semin. Cell Dev. Biol.* **22**, 729–734 [CrossRef](#) [Medline](#)
30. Allen, B. L., and Taatjes, D. J. (2015) The Mediator complex: a central integrator of transcription. *Nat. Rev. Mol. Cell Biol.* **16**, 155–166 [CrossRef](#) [Medline](#)
31. Jeronimo, C., and Robert, F. (2017) The Mediator complex: at the nexus of RNA polymerase II transcription. *Trends Cell Biol.* **27**, 765–783 [CrossRef](#) [Medline](#)
32. Zhao, X., Xiaoli, Zong, H., Abdulla, A., Yang, E. S., Wang, Q., Ji, J. Y., Pessin, J. E., Das, B. C., and Yang, F. (2014) Inhibition of SREBP transcriptional activity by a boron-containing compound improves lipid homeostasis in diet-induced obesity. *Diabetes* **63**, 2464–2473 [CrossRef](#) [Medline](#)
33. Jin, C., Strich, R., and Cooper, K. F. (2014) Slt2p phosphorylation induces cyclin C nuclear-to-cyttoplasmic translocation in response to oxidative stress. *Mol. Biol. Cell* **25**, 1396–1407 [CrossRef](#) [Medline](#)
34. Willis, S. D., Stieg, D. C., Ong, K. L., Shah, R., Strich, A. K., Grose, J. H., and Cooper, K. F. (2018) Snf1 cooperates with the CWI MAPK pathway to mediate the degradation of Med13 following oxidative stress. *Microbial Cell* **5**, 357–370 [CrossRef](#) [Medline](#)
35. Onoyama I., Suzuki, A., Matsumoto, A., Tomita, K., Katagiri, H., Oike, Y., Nakayama, K., and Nakayama, K. I. (2011) Fbxw7 regulates lipid metabolism and cell fate decisions in the mouse liver. *J. Clin. Invest.* **121**, 342–354 [CrossRef](#) [Medline](#)
36. Puertollano, R. (2014) mTOR and lysosome regulation. *F1000prime Rep.* **6**, 52 [CrossRef](#) [Medline](#)
37. Song, Z., Xiaoli, A. M., Zhang, Q., Zhang, Y., Yang, E. S. T., Wang, S., Chang, R., Zhang, Z. D., Yang, G., Strich, R., Pessin, J. E., and Yang, F. (2017) Cyclin C regulates adipogenesis by stimulating transcriptional activity of CCAAT/enhancer-binding protein α . *J. Biol. Chem.* **292**, 8918–8932 [CrossRef](#) [Medline](#)
38. Nagata, T., Redman, R. S., and Lakshman, R. (2010) Isolation of intact nuclei of high purity from mouse liver. *Anal. Biochem.* **398**, 178–184 [CrossRef](#) [Medline](#)